Effect of Chemical Treatment on Electrical Conductivity, Infrared Absorption, and Raman Spectra of Single-Walled Carbon Nanotubes

V. Skákalová, A. B. Kaiser,† U. Dettlaff-Weglikowska, K. Hrnčariková,‡ and S. Roth

Max Planck Institute for Solid State Research, Heisenbergstr. 1, 70569 Stuttgart, Germany, MacDiarmid Institute for Advanced Materials and Nanotechnology, SCPS, Victoria University of Wellington, P. O. Box 600, Wellington, New Zealand, and Slovak Technical University, Faculty of Chemical Technology, Radlinského 9, 81237 Bratislava, Slovakia

Received: November 18, 2004; In Final Form: January 7, 2005

We investigate the magnitude and temperature dependence of electrical conductivity, the optical and infrared absorption, and the Raman spectra of single-walled carbon nanotube (SWNT) bucky-paper after chemical treatment and determine the correlations between the changes in these properties. Ionic-acceptor doping of the SWNT bucky-paper (with $SOCl_2$, iodine, H_2SO_3, etc.) causes an increase of electrical conductivity that correlates with an increase of the absorbance in the far-IR region and an increase in the frequency of Raman spectral lines. Conversely, treatment with other molecules (e.g., aniline, $PyPhF_5$, $PhCH_2Br$, etc.) leads to a decrease in both conductivity and far-IR absorption. The temperature dependence of the conductivity gives a good indication of the presence of metallic charge carriers and is in agreement with the model of interrupted metallic conduction.

Introduction

Most current methods for preparing single-walled carbon nanotubes (SWNTs) lead to a material that not only contains a mixture of nanotubes of different diameters and chiralities but also different carbonaceous impurities such as amorphous carbon, graphitic particles, and other carbon nanoparticles. Chemical treatment is necessary to achieve purity[1−3] and to dissolve bundles of SWNTs,[4−7] and in many cases, this processing introduces defects in the SWNTs. For some electronic applications, delocalized electronic states in the SWNTs are required, so strong covalent bonds between SWNTs and other molecules that lead to localization of the SWNT electronic states should be avoided; the electronic properties of the nanotubes can be changed by doping or intercalation,[8−17] for example, for use in sensors.[18] For other applications, a specific functionalization involving covalent chemistry is required, for example, to create cross-links between SWNT,[19] to form T-junctions of individual SWNTs,[20] to fix SWNTs into a polymer matrix in composites,[21] for some methods to separate the metallic SWNT from semiconducting ones,[22−26] and for many other requirements. It is therefore of great interest to investigate the effects of different chemical treatments in modifying the electronic properties of SWNTs and to determine the systematic changes due to each type of treatment.

Recently, some progress in the field has been reported in the work of Hu et al.[27] Their results showed that sidewall functionalization of SWNT by dichlorocarbene led to suppression of the van Hove peaks in the IR region of the absorbance spectrum and to a strong decrease in the far-IR (FIR) absorbance. This decrease contrasted strongly with the increase in FIR absorbance produced by treatment with the acceptor dopant bromine. Thus, it appeared that the change in the FIR spectrum could clearly distinguish whether the chemical treatment leads to the formation of a strong covalent bond (a decrease in FIR absorbance) or an ionic interaction between the reagent and the SWNT (an increase in FIR absorbance). But this criterion can only distinguish between ionic *acceptor* doping and covalent bonding, because we show in this paper that donor dopants supply electrons that appear to fill in the hole states at the Fermi level of the pristine nanotubes and cause a reduction in the FIR absorption that is similar to that caused by covalent bonding. We do, however, find some difference in suppression of the Van Hove peaks between ionic-donor doping and covalent bonding, as expected.[27]

One of the main purposes of the paper is to make a detailed investigation of the temperature-dependent conductivity for SWNTs exposed to different chemical treatments, as well as to relate changes in conductivity to changes in optical and Raman spectra in order to understand the effects of acceptor and donor dopants and of covalent bonding. We also compare our results with those of other authors who altered the properties of SWNTs by electrochemical charging[28] or by applying a counter electrode gate voltage.[29]

The electrochemical studies of Kavan et al.[28] showed that electrochemical charging strongly modifies the Van Hove absorbance peaks of SWNTs and also leads to changes in the frequency of the tangential mode (TM) in the Raman spectrum. Interestingly, our results for changes in Raman spectra due to acceptor and donor dopant molecules show qualitatively similar behavior. Kavan et al.[28] did not measure the absorbance below 0.55 eV and so did not investigate the effect of electrochemical charging on metallic carriers in nanotubes.

Very recently, Wu et al.[29] measured the transmittance of transparent, conductive SWNT films as the charge on the nanotubes was changed by applying a negative or positive counter electrode gate voltage. They found that the FIR transmittance and the S_{11} van Hove dip in the transmittance could each be enhanced or diminished depending on the sign of the gate voltage. In this paper, we show that an analogous

† MacDiarmid Institute for Advanced Materials and Nanotechnology.
‡ Slovak Technical University.

10.1021/jp044741o CCC: $30.25
Published on Web 03/19/2005

pattern of increases and decreases in the FIR absorbance of SWNTs arises from dopants of different types (acceptor and donor). However, an analogous increase in the S_{11} van Hove absorbance peak is not observed.

Experimental Section

Sample Preparation. Purified SWNTs produced by the HiPCO method at CNI, Houston (U.S.A.), were used for further treatment. The bucky-paper was prepared by ultrasonication of the nanotubes suspension in SDS solution and subsequent vacuum filtration on a membrane polycarbonate filter.

The Chemical Treatments Were Performed as Follows:

Thionyl chloride. $SOCl_2$ (99% purity) was purchased from Fluka AG (Switzerland). The bucky-paper filtered from the suspension of SWNTs with SDS water was treated in $SOCl_2$ at 45 °C. The time of treatment was 10 h. Experiments with $SOCl_2$ treatment showed that there was no difference in the effect on the electrical conductivity when the bucky-paper was prepared from the $SOCl_2$-treated powder or when the bucky-paper was treated directly. We expect this similarity for any ionic treatment.

Iodine. Doping was performed by treating the bucky-paper in a solution of iodine in toluene for 10 days. Afterward, the sample was dried in a stream of argon.

H_2SO_3. A piece of bucky-paper (14 mg) has been treated with 5% solution of H_2SO_3 in water at 60 °C for 1 h and dried at room temperature.

H_2SO_4. A powder of SWNTs (26 mg) was stirred with 2 mL of 96% H_2SO_4 and 2 mL of acetic acid anhydride at 60 °C for 4 h. The bucky-paper obtained after filtration of the slurry was washed with acetic acid anhydride and dried at 105 °C.

SO_2Cl_2. A powder of SWNTs (20 mg) has been stirred with 10 mL of SO_2Cl_2 at 60 °C for 24 h. The bucky-paper obtained after filtration has been dried at room temperature.

Aniline. A powder of SWNTs (25 mg) was stirred in 5 mL of aniline under reflux for 3 days. The dense slurry was then filtered on a nylon membrane filter (pore size 5 μ) and washed with 2-propanol.

Ethylenediamine (EDA). A powder of SWNTs (12 mg) was stirred with 12 mL of ethylenediamine at 60 °C for 18 h. The bucky-paper formed after filtration was dried at 105 °C.

$PyPhF_5$. A powder of SWNTs (20.09 mg) were stirred in *o*-dichlorobenzene (100 mL). Perfluorophenyl-1*H*-pyrrole in *o*-dichlorobenzene (10 mL) was added and heated at 160 °C for 45 min, then diluted by Et_2O (50 mL) and DMSO (100 mL). After filtration and drying, 17.37 g of functionalized SWNTs were obtained.

$PhCH_2Br$. A powder of SWNTs (20.33 mg) were stirred in toluene (100 mL); benzylbromide (7.19 g, 42.0 mmol) was added and the mixture refluxed for 8 h. After filtration and washing in toluene (20 mL), 20.01 g of functionalized SWNTs were obtained.

$PhCH_2Cl$. A powder of SWNTs (20.67 mg) were stirred into toluene (100 mL); benzyl chloride (5.32 g, 42.0 mmol) was added and the mixture refluxed for 8 h. After filtration and washing in toluene (20 mL), we obtained 19.7 g of functionalized SWNTs.

Electrical Conductivity Measurements. Electrical conductivity was measured using the four-probe method. The contacts were formed by silver paint. The sample was placed in a long tube filled with helium gas. For the temperature dependence measurement, the tube was fixed into a liquid helium bottle.

Optical Absorption Spectroscopy. Optical absorption and IR spectra were measured by evaporating a drop of SWNT suspension in CCl_4 on a KBr pellet. For optical spectroscopy, a UV−vis/near-IR Perkin-Elmer Lambda spectrometer was used. The IR spectra were measured by a Bruker IFS66 spectrometer.

Raman Spectroscopy. Raman spectra were measured using microscope laser Raman spectroscopy with a Jobin Yvon−LabRam spectrometer. The laser excitation wavelength was 632 nm with spectral resolution of 4 cm^{-1}.

TABLE 1: Conductivities of Bucky-Paper Chemically Treated with Molecules that Increase Conductivity

SWNT +	pristine	$SOCl_2$	H_2SO_3	iodine	H_2SO_4	SO_2Cl_2
conductivity (S/cm)	550	3000	1460	1450	900	820

TABLE 2: Conductivities of Bucky-Paper Chemically Treated with Molecules that Decrease Conductivity

SWNT +	pristine	$PyPhF_5$	aniline	EDA	$PhCH_2Br$	$PhCH_2Cl$
conductivity (S/cm)	550	37	70	80	130	400

Results and Discussion

The values of the electrical conductivity of SWNT bucky-paper after various chemical treatments at room temperature are given in two separate tables. Table 1 features the molecules that cause an enhancement of the value of electrical conductivity compared to the pristine sample, while Table 2 presents those molecules that cause a decrease in electrical conductivity upon chemical treatment.

The occurrence of a positive or negative change in the electrical conductivity reflects the character of the interaction between the SWNTs and a specific molecule. We illustrate this by demonstrating the correlation between the change of electrical conductivity and the features in the IR absorption and Raman spectra, discussing separately the case when the conductivity was increased and the case when it was decreased.

Optical Absorption Spectroscopy (Conductivity Increase). Figure 1 demonstrates the optical absorption spectra of SWNTs chemically treated with some of the molecules from Table 1 ($SOCl_2$, H_2SO_3, I_2, and H_2SO_4) compared to the spectrum of the pristine sample. For all the dopants presented in Figure 1, the following common features after doping can be observed:

(i) The peak at 0.83 eV, identified[27] with the S_{11} interband transition between the first pair of Van Hove singularities of the semiconducting tubes, decreases (and disappears for $SOCl_2$ doping). The small peak near 1.5 eV, identified with the S_{22} interband transition between the second pair of Van Hove singularities of the semiconducting tubes, shows similar behavior.

(ii) The minimum of the curve, which for the pristine HiPCO−SWNT is at 0.39 eV, shifts to higher energies (to 0.66 eV for $SOCl_2$ doping).

(iii) The absorption significantly increases at low energies (below 0.5 eV).

These observations represent a shift toward more metallic behavior of the SWNT bucky-paper. The increased FIR absorbance signals the presence of an increased density of charge carriers near the Fermi level, as expected from the increase of conductivity (by a factor of 5 for $SOCl_2$ doping). A strong increase in FIR absorbance was observed by Hu et al.[27] for SWNTs treated with bromine, an acceptor dopant. The removal of electrons from the nanotubes by acceptor dopants lowers the Fermi level and can thereby create more holes in the valence band of semiconducting nanotubes. Besides increasing the conductivity, the depletion of filled states in the lower Van Hove singularity also lessens the interband transitions (S_{11}) between

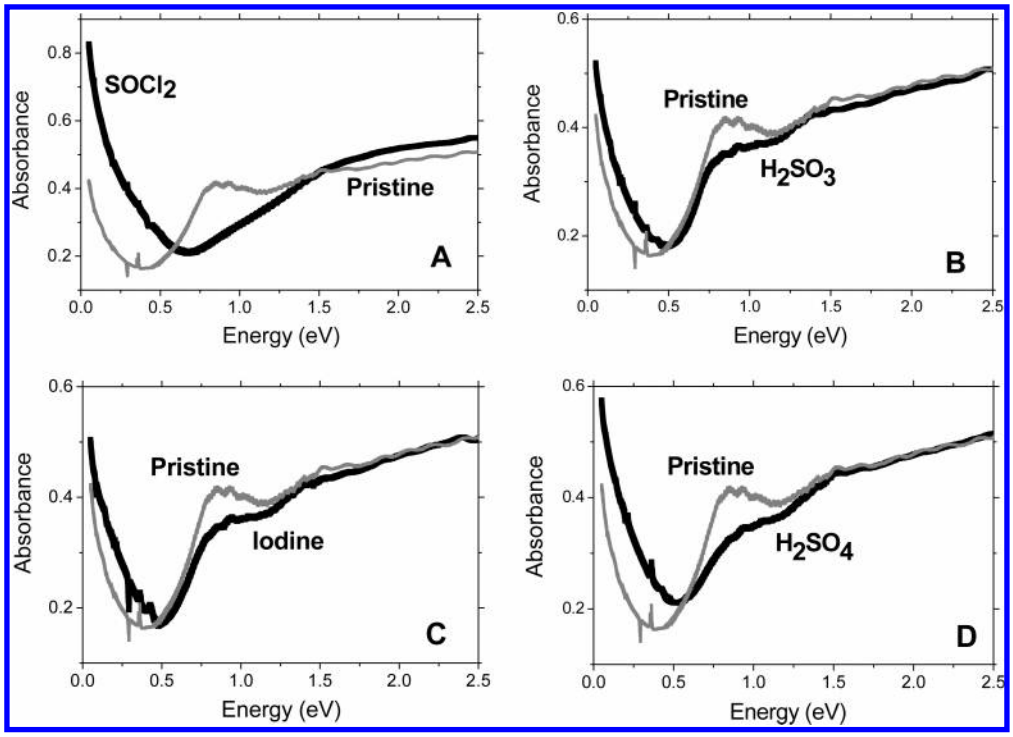

Figure 1. Optical absorption spectra of the $SOCl_2$-doped (A), H_2SO_3-doped (B), iodine-doped (C), and H_2SO_4-doped (D) SWNT, compared to pristine SWNT.

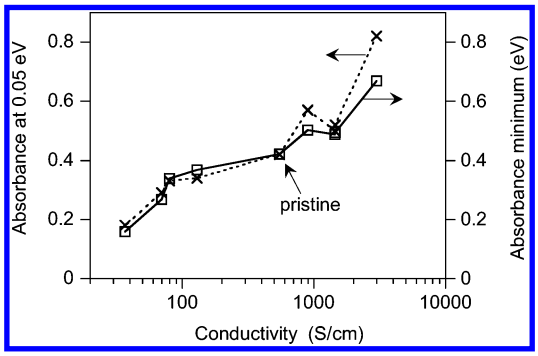

Figure 2. FIR absorbance at an energy of 0.05 eV and absorbance minimum position in energy plotted as a function of the electrical conductivity (logarithmic scale) for SWNT bucky-papers treated with (from right) $SOCl_2$, H_2SO_3, iodine, H_2SO_4, pristine sample, $PhCH_2Br$, EDA, aniline, and $PyPhF_5$. (The fact that absorbance at 0.05 eV is 0.42 and its energy at minimum is 0.42 eV for the pristine sample is coincidental.)

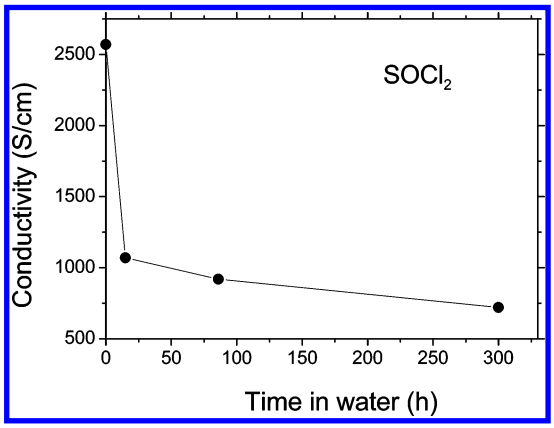

Figure 3. Decrease of conductivity of the $SOCl_2$-doped SWNT bucky-paper as a function of rinsing time in water (for a different sample than the one reported in Table 1).

the first pair of Van Hove singularities in semiconducting nanotubes,[27] which would contribute to the decrease in the first Van Hove peak in the absorbance that we observe. The other main feature that we see (the shift of the minimum in the absorbance to higher energies) is largely a result of the increase in the FIR absorbance. This is illustrated in Figure 2 where we see that the shift of the minimum is closely correlated with the increase of the measured absorbance at 0.05 eV.

There is a clear parallel between the interpretation of our data in terms of changes in the density of mobile holes and the observations of Wu et al.[29] for SWNT thin films. These authors changed the density of holes by varying a counter electrode gate voltage rather than by adding dopants. For negative gate voltages (which attracted holes onto the nanotubes in analogy to the acceptor doping of our samples), they found that, in the IR region around 3000 nm (0.41 eV), the transmittance decreased (corresponding to the absorbance increase in our case). They also measured a suppression of the S_{11} transmittance dip for this positive charging of the nanotubes (corresponding to the suppression of the S_{11} absorbance peak that we observe).

There is no doubt that iodine acts as an ionic dopant in SWNTs.[15] However, there are still discussions about the chemistry for $SOCl_2$ doping. If the interaction between $SOCl_2$ and SWNTs is ionic, it should be easy to remove the ions from the host SWNT just by rinsing in water. The result of this experiment is shown in Figure 3. $SOCl_2$-doped bucky-paper was rinsed in deionized water at room temperature for a certain time, dried in air, and the electrical conductivity was measured for different times. The value of the conductivity decreases dramatically: In 15 h, the original enhancement of the conductivity due to doping is reduced from a factor of 5 to 2, and a further decrease occurs for longer times. This result strongly supports an ionic character for the interaction between the $SOCl_2$ dopant and the SWNTs.

Optical Absorption Spectroscopy (Conductivity Decrease). Figure 4 shows the optical absorption spectra of the SWNTs chemically treated with some of the molecules from Table 2 ($PyPhF_5$, aniline, EDA, and $PhCH_2Br$) compared to the spectrum

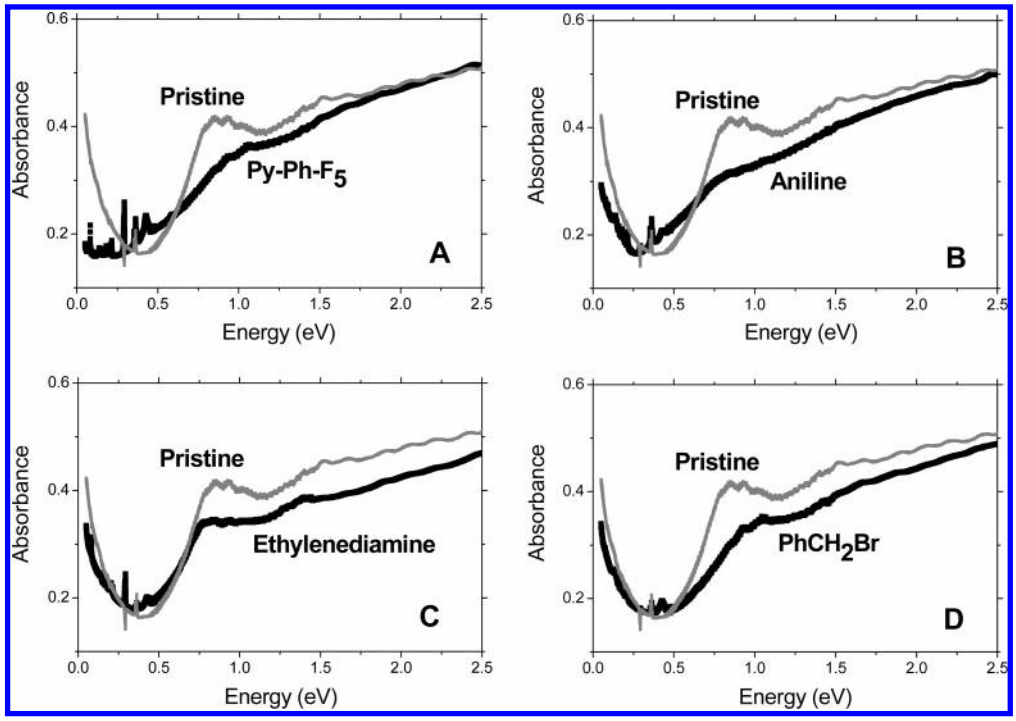

Figure 4. Optical absorption spectra of the SWNT treated with $PyPhF_5$ (A), aniline (B), EDA (C), and $PhCH_2Br$ (D), compared to pristine SWNT.

of the pristine sample. For these molecules, as the conductivity becomes lower (see Table 2), the following trends can be observed (Figure 4):

(i) The S_{11} and S_{22} interband transitions between pairs of Van Hove singularities decrease (and almost disappear for aniline doping).

(ii) The minimum of the curve (for the pristine HiPCO−SWNT at 0.39 eV) shifts to lower energies, while the absorbance in the low-energy region decreases (a change toward less metallic behavior, clearly consistent with the decrease of conductivity in these cases).

The interpretation of these observations is more complex than for the previous case of acceptor dopants that increase conductivity. First, molecules that form covalent bonds with the SWNT sidewalls can cause severe disruption of the electronic structure and suppression of both the FIR absorbance and the S_{11} and S_{22} interband transitions, as found by Hu et al.[27] for dichlorocarbene functionalization of SWNTs. In this case, metallic tubes are likely to be more reactive, having low-energy electrons available for a chemical reaction.[26] The covalent bonds form sp^3-electron states, interrupting the delocalization of the planar π-system and depleting the metallic states at the Fermi level.[27]

Second, we expect that ionic dopants could also *decrease* conductivity. This is because the pristine SWNTs have a significant conductivity ascribed to acceptor-doping by oxygen in air: Upon donor doping up to a certain concentration, the electrons will fill the existing hole states in the valence band, decreasing the concentration of charge carriers and so the conductivity. A demonstration of the analogous reduction of charge-carrier density by a positive counter electrode gate voltage (which attracted electrons onto the nanotubes) was very recently provided by Wu et al.,[28] who observed an increase in the transmittance around 0.41 eV (corresponding to the decrease in FIR absorbance in our case).

Our data appear to demonstrate both mechanisms for the reduction in conductivity. Of the five molecules leading to a reduction in conductivity (Table 2), two appear to show ionic dopant character (EDA and $PyPhF_5$), and three appear to show covalent bonding character (aniline, $PhCH_2Br$, and $PhCH_2Cl$). This is illustrated by Table 3, which shows the comparison of the electrical conductivity of these samples measured before and after they were rinsed in water for 10 h at room temperature and then dried. It is likely that rinsing in water can remove from the SWNTs bucky-paper molecules interacting as ions more easily than those covalently bound. The reduced concentration after rinsing will lead to a partial recovery of the electrical conductivity, closer to that of the pristine state. The remarkable increase of the conductivity after rinsing indicates that $PyPhF_5$ and EDA in the presence of nanotubes are likely to act as donor ions. On the other hand, the fact that the conductivity of the samples treated with aniline, $PhCH_2Br$, and $PhCH_2Cl$ exhibits a slight decrease after rinsing in water suggests that these molecules form covalent bond with SWNTs.

TABLE 3: Effect of Rinsing in Water on Conductivity of Treated Bucky-Paper

SWNT +	$PyPhF_5$	aniline[a]	EDA	$PhCH_2Br$	$PhCH_2Cl$[a]
conductivity before rinsing (S/cm)	37	32	80	130	250
conductivity after rinsing (S/cm)	150	24	212	120	200

[a] In the case of aniline and $PhCH_2l$, we used a different sample for this experiment from that examined in the previous measurements, so the conductivity values differ from those shown in Table 2.

Examining the changes in FIR absorbance in Figure 4 and the relation to conductivity in Figure 2, we see no obvious difference between the ionic-donor dopants (EDA and $PyPhF_5$) and the covalent-bonding dopants (aniline and $PhCH_2Br$). It therefore appears that the effect on FIR absorbance is determined largely by the decrease in hole density regardless of whether that reduction arises from donor doping or from covalent bonding.

One would expect a greater difference between the ionic and covalent interactions with the SWNTs in their effect on the S_{11} and S_{22} interband transitions. The severe disruption of the electronic band structure by covalent bonding leads to strong suppression of all the interband transitions.[27] While the ionic-

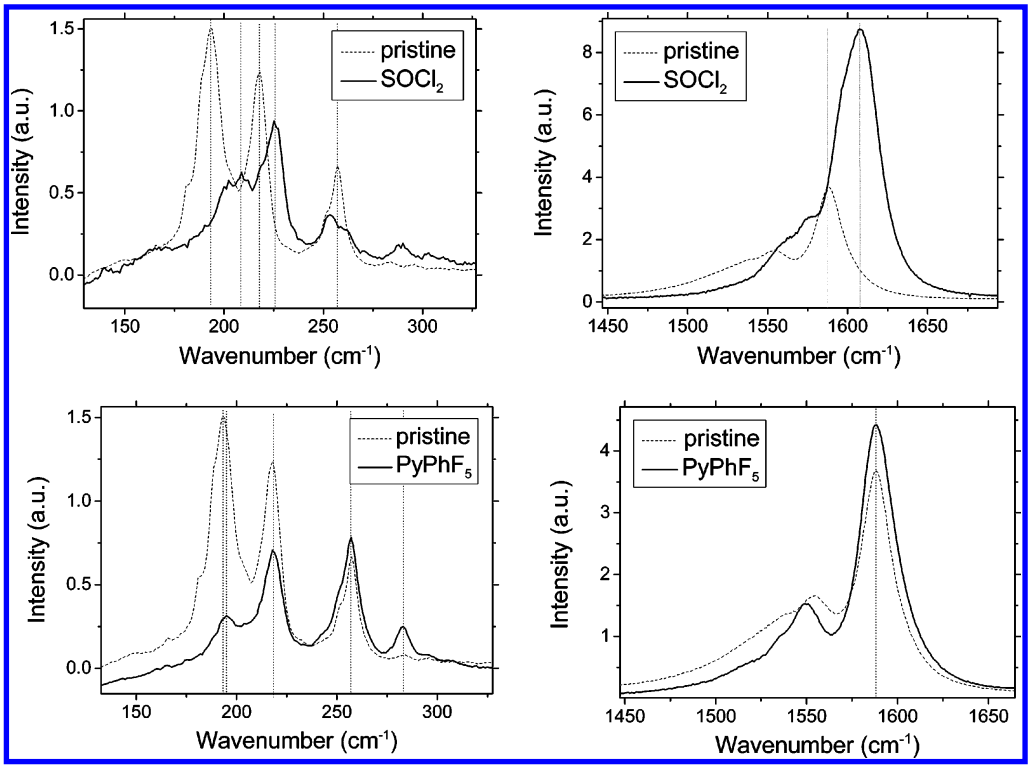

Figure 5. Raman RBM and tangential mode spectra for SWNTs treated with $SOCl_2$ (upper panels) and $PyPHF_5$ (lower panels) compared to the pristine sample (dotted lines) (these two molecules produced the largest conductivity increase and decrease, respectively).

donor dopants will also have some disruptive effect, they will also restore the electron filling of the lower Van Hove singularities and thus tend to restore the S_{11} and S_{22} interband transition absorbance peaks. This restoration effect in the S_{11} and S_{22} interband transitions has been clearly seen by Wu et al.[29] for negative charging of the SWNTs by a positive gate voltage, and also (to a lesser extent) by Kavan et al.[28] for negative electrochemical charging.

However, we find no increase in the S_{11} and S_{22} interband transition absorbance peaks for donor doping; the analogy between our results and those of Wu et al.[29] breaks down for the Van Hove peaks. Our data in Figure 4 do however suggest that the suppression of the interband peaks in our absorbance data for aniline is slightly greater than for $PyPhF_5$ that has lower conductivity and so has smaller hole density, and likewise, the overall peak suppression for covalently bonded $PhCH_2Br$ is slightly greater than for the donor dopant EDA that has lower conductivity. Hence, the extent of suppression of the S_{11} and S_{22} peaks does not follow the conductivity decrease but suggests a greater effect from covalent bonding than from ionic doping, as expected. A likely reason for the discrepancy between the effect of our donor doping molecules and that for electrochemical[28] or gate voltage[29] charging is that our donor dopant molecules disrupt the electronic structure much more than electrochemical or gate voltage charging, thereby decreasing rather than increasing the interband transitions.

The data for the decrease in FIR absorbance and the shift of the absorbance minimum for the molecules in Table 2 that decrease conductivity are also included as a function of conductivity in Figure 2. It is clear that FIR absorbance is still very sensitive to the smaller absolute changes in conductivity produced by these molecules compared to the large increase to 3000 S/cm for $SOCl_2$. We shall see below that this is not the case for changes in the Raman spectral lines.

Raman Spectroscopy. We give examples of the Raman spectra for our samples by showing in Figure 5 the spectra for the pristine SWNT sample and for SWNTs with $SOCl_2$ and $PyPHF_5$ added (these molecules produced the largest conductivity increase and decrease, respectively). We note a trend for the magnitude of the Raman line for the lower radial breathing modes (RBM) near 200 and 220 cm^{-1} to decrease on addition of molecules, while the mode for the narrower tubes near 285 cm^{-1} strongly increased; these trends are illustrated by the examples for $PyPHF_5$ and $SOCl_2$ in Figure 5. For $SOCl_2$, there are large shifts in peak energies, and peak splitting appears to occur, possibly due partly to morphological effects as a result of doping.[30] Those molecules that produced an increase in conductivity also produced a large increase in the magnitude of the tangential mode (TM) lines (for example, see the $SOCl_2$ data in Figure 5), whereas decreasing conductivity produced little change in the TM lines. Aniline deviated from the pattern of the other molecules by producing an enhanced Raman line at 224 cm^{-1} and a broad band around 1300 cm^{-1} that makes it impossible to identify the D line.

In Figure 6, we show the magnitude of the Raman shifts for all samples measured. The frequency of the Raman lines plotted for each sample in ascending order of dc conductivity does show systematic behavior except for aniline, which tends to produce larger Raman shifts than other molecules giving similar conductivity (but not for the TM line at 1590 cm^{-1}). Because the aniline data are affected by the presence of additional features arising from the aniline molecules and show anomalous behavior, we indicate the aniline points by open squares and omit them from the trend line joining data points.

The main feature of Figure 6 is the unmistakable trend for the Raman shift to increase for the samples with the highest conductivity (essentially those with $SOCl_2$ and H_2SO_3 doping). The greater hole-carrier density in these samples is associated with a stiffening of the modes.[31] This is true for the RBM lines between 190 and 290 cm^{-1}, the TMs near 1590 cm^{-1}, and the D and 2D lines near 1310 and 2615 cm^{-1}. The Raman shifts for the other molecules (apart from aniline) show little change

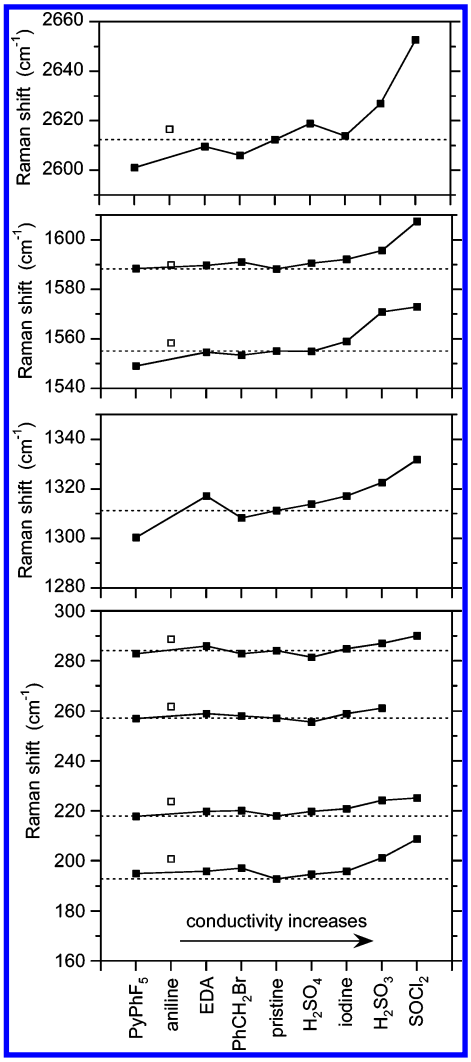

Figure 6. Raman shift of the RBM, D, G, and 2D lines for SWNTs chemically treated with different molecules as listed, compared to the values for the pristine sample (dotted lines); the order of samples along the horizontal axis is that of increasing conductivity as given by Tables 1 and 2. Aniline data (open squares) are not included in the trend lines (see text for discussion).

from those of the pristine sample: there is a slight indication of a decrease of the Raman shifts for the $PyPhF_5$ molecule.

This behavior has a remarkable similarity to the observations of Kavan et al.[28] for electrochemical charging of SWNTs. These authors found that the Raman shift of the 1590 cm^{-1} TM mode increased up to approximately 1610 cm^{-1} if holes are introduced into the SWNTs. These authors also observed a threshold effect as we do: the Raman shift of the 1590-cm^{-1} TM mode intially increased very little with applied potential and then increased much more rapidly than expected for voltages between 1.0 and 1.6 V, in analogy to our sharp increase for $SOCl_2$ and H_2SO_3 doping that led to conductivities of around 1500 S/cm or greater. A somewhat similar threshold effect (with a larger threshold voltage) was seen for negative electrochemical charging of SWNTs,[28] in analogy to our small effect for donor doping. Our case is, of course, more complex owing to the presence of the dopant molecules, but the analogy does support the interpretation of our data (except for aniline) in terms of the changes in hole-carrier density. In addition, we note that the slightly asymmetric broadening of the 1590-cm^{-1} TM mode for $SOCl_2$ doping shown in Figure 5 resembles that found[28] for electrochemical charging of SWNTs produced by the HiPCO process and ascribed to Breit−Wigner−Fano broadening due to the density of free holes

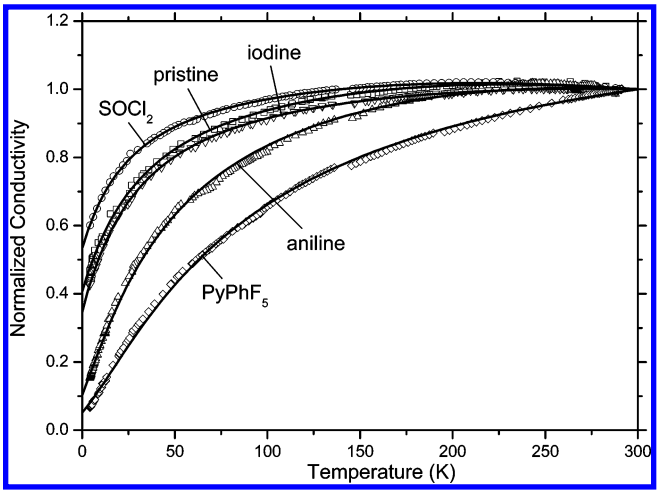

Figure 7. Electrical conductivity of pristine SWNT bucky-paper and after treatment with $SOCl_2$, iodine, aniline, and $PyPhF_5$ (normalized by its extrapolated value at a temperature of 300 K to show the relative temperature dependences). The lines are fits to eq 1 for the interrupted metallic conduction model, with fit parameters listed in Table 4.

(the presence of additional Raman lines from metallic nanotubes may also play a role[32]).

Temperature Dependence of DC Conductivity. The behavior of the dc conductivity at low temperatures is an important indicator of metallic or semiconducting behavior and of mechanisms of conduction. We have therefore measured the influence of different chemical treatments (two that increase and two that decrease conductivity) on the temperature dependence of the electrical conductivity of SWNT bucky-paper down to low temperatures. Our data are shown in Figure 7. Iodine produces no significant change in the temperature dependence, whereas $SOCl_2$ yields a smaller relative decrease of conductivity as temperature decreases. Both the molecules that decrease conductivity lead to an increase in the relative temperature dependence.

There is clear evidence for metallic behavior. The low-temperature conductivities extrapolate to nonzero values in the zero-temperature limit, which is a key signature of free charge carriers that require no thermal activation (i.e., of metallic behavior). For the $PyPhF_5$ data, the extrapolated conductivity intercept in the $T = 0$ limit is very small but still nonzero, in agreement with the presence of the very small upturn in FIR absorbance at low energies shown in Figure 4.

Another sign of metallic behavior is the shallow peak in conductivity and the changeover to a negative metallic sign for the conductivity temperature dependence above 250 K (this changeover does not occur for the $PyPhF_5$ data, at least not below 300 K). However, the dominant sign of the temperature dependence (from 200 K down to low temperatures) is nonmetallic.

This mixed metallic−nonmetallic behavior in the conductivity is not consistent with simple parallel conduction in metallic and semiconducting nanotubes, because in this case, we would expect an exponential-type semiconductor conductivity term that dominates at higher temperatures (which, in fact, is where we find that the conductivity temperature dependence changes to metallic).

The general behavior of our data is similar to the pattern of conductivity temperature dependence seen in SWNT networks and in highly conducting organic polymers as disorder and doping levels are changed.[33,34] This pattern can be accounted for in terms of metallic conduction interrupted by small barriers through which tunneling occurs. In the case of nanotube

TABLE 4: Fit Parameters for Conductivity Temperature Dependence (Figure 7)

SWNT +	$PyPhF_5$	aniline	pristine	iodine	$SOCl_2$
k_BT_b (meV)	7.3	3.9	2.0	1.9	1.3
T_s/T_b	0.31	0.40	0.98	0.87	1.4

networks, the barriers are twists or other defects along the nanotubes, intertube or interbundle contacts; such barriers typically dominate the resistance. One form of the expression for the resistivity given by this model that accounts for several previous data sets for SWNT networks is[33,35,36]

$$\rho(T) = \frac{1}{\sigma(T)} = A \exp\left(-\frac{T_m}{T}\right) + B \exp\left(\frac{T_b}{T_s + T}\right) \qquad (1)$$

where the geometrical factors A and B can be taken as constant. The first term is for quasi-one-dimensional metallic conduction involving the suppression of resistivity at lower temperatures where carriers are not easily backscattered (for scattering by lattice vibrations, k_BT_m would be the energy of the backscattering phonons[37]). The second term represents fluctuation-assisted tunneling[38] through barriers, with the order of magnitude of typical barrier energies indicated by the value of k_BT_b and the extent of the decrease of conductivity at low temperatures indicated by the ratio T_s/T_b. The interplay between the metallic and nonmetallic terms accounts for the conductivity maximum often seen in SWNT networks or in conducting polymers. We obtain good fits to the data in Figure 7 by using $T_m = 1000$ K[35] with fit parameters k_BT_b and T_s/T_b listed in Table 4. The metallic temperature dependence is too limited to derive accurate values for the contribution of the temperature-dependent metallic term to the total resistivity at 300 K, but this fraction is only a few percent (and approximately zero for $PyPhF_5$). As expected, the barrier parameter k_BT_b increases as conductivity decreases, while the ratio T_s/T_b decreases as the conductivity decrease at low temperatures becomes more pronounced (i.e., as the samples show less metallic character). The small values of T_s/T_b and of the low-temperature conductivity for $PyPhF_5$, and the very small upturn in low-energy FIR absorbance, suggest that delocalized metallic carriers are almost eliminated, and it is on the verge of becoming a disordered semiconductor; such a transition is seen in conducting polymers as the doping level and free-carrier density decrease to low values.[34] For aniline, the presence of an almost constant conductivity at higher temperatures and a FIR low-energy upturn only slightly lower than that of the pristine sample suggest that the hole-carrier density is not greatly diminished and conductivity is decreased more strongly by disorder scattering; this is consistent with covalent bonding creating considerable disorder but less direct effect on carrier density than donor doping.

Conclusion

We have shown that there are close correlations of the changes in several properties when SWNTs undergo chemical treatments involving exposure to different types of molecules.

(1) An increase in conductivity correlates with an increase in the FIR absorbance as charge-carrier density is increased by acceptor dopant molecules, and conversely, a decrease in both properties occurs for donor dopants or covalent bonding molecules (as summarized in Figure 2). Our results demonstrate an analogy to changes in conductivity due to charging of nanotubes positively or negatively by a counter electrode gate voltage.[29] The conductivity is therefore a sensitive probe of the charging of the SWNTs that is easy to measure and effective for both high and low charge densities.

(2) A decrease of the S_{11} and S_{22} interband absorbance peak due to transitions between the first pair of Van Hove singularities for semiconducting tubes is found for all molecules (Figures 1 and 4). The peak disappears for $SOCl_2$ doping (which gives the highest conductivity). The suppression of peaks for aniline and $PhCH_2Br$ that appear to bond covalently with the nanotubes is slightly greater than the decrease for donor dopants of lower conductivity ($PyPhF_5$ and EDA, respectively), confirming greater disruption of the band structure by covalent bonding, as expected.[27] In contrast to the FIR absorbance, the effect on the S_{11} peak of our donor doping is different from that of adding electrons to the nanotubes by a counter electrode gate voltage[29] or electrochemical charging;[28] both of these charging mechanisms led to an *increase* in the S_{11} peak. We ascribe this difference to a minimal disruptive effect on the band structure due to gate or electrochemical charging as compared to donor dopants.

(3) There is a shift of the RBM, TM, D, and 2D Raman spectral lines to higher frequencies for the acceptor dopants that yield the highest conductivities (Figure 6), but little change for the other dopants (possibly a decrease in frequency for the lowest conductivity sample). Thus, the Raman shifts appear less sensitive to changing carrier densities than FIR absorbance. A somewhat analogous "threshold" effect was also seen[28] for electrochemical charging of SWNTs.

(4) The temperature dependence of the dc conductivity (Figure 7) confirms the presence of metallic charge carriers in the SWNTs. This temperature dependence is described well by the model of metallic conduction interrupted by barriers (defects or intertube contacts) that was developed[34] to understand conduction in conducting polymers and SWNT networks. There is a trend for a stronger percentage decrease in conductivity as the temperature is lowered for samples of lower conductivity, and the lowest conductivity sample appears on the verge of a metal−semiconductor transition.

In summary, the changes in properties as a result of chemical treatment that we describe provide some additional means of understanding the results of chemical treatments.

Acknowledgment. This work was supported by the EU project SPANG no. NMP4-CT-2603-505483, project Kompetenznetz Funktionalle Nanostrukturen of State Baden-Wuertemberg, and a grant of the Slovak Ministry of Education VEGA 1/0055/03.

References and Notes

(1) Shelimov, K. B.; Esenaliev, R. O.; Rinzler, A. G.; Huffman, C. B.; Smalley, R. E. *Chem. Phys Lett.* **1998**, *282*, 429−434.

(2) Hu, H.; Zhao, B.; Itkis, M. E.; Haddon, R. C. *J. Phys. Chem. B* **2003**, *107*, 13838−13842.

(3) Itkis, M. E.; Perea, D. E.; Nijogy, S.; Rickard, S. M.; Hamon, M. A.; Hu, H.; Zhao, B.; Haddon, R. C. *Nano Lett.* **2003**, *3*, 309−314.

(4) Dieckmann, G. R.; Dalton, A. B.; Johnson, P. A.; Razal, J.; Chen, J.; Giordano, G. M.; Munoz, E.; Musselman, I. H.; Baughman, R. H.; Draper, R. K. *J. Am. Chem. Soc.* **2003**, *125*, 1770−1777.

(5) Zorbas, V.; Ortiz-Acevedo, A.; Dalton, A. B.; Yoshida, M. M.; Dieckmann, G. R.; Draper, R. K.; Baughman, R. H.; Jose-Yacaman, M.; Musselman, I. H. *J. Am. Chem. Soc.* **2004**, *126*, 7222.

(6) Strano, M. S.; Doorn, S. K.; Haros, E. H.; Kittrell, C.; Hauge, R. H.; Smalley, R. E. *Nano Lett.* **2003**, *3*, 81.

(7) Shaffer, M. S. P.; Fan, X.; Windle, A. H. *Carbon* **1998**, *36*, 1603−1612.

(8) Kazaoui, S.; Minami, N.; Jacquemin, R.; Kataura, H.; Achiba, Y. *Phys. Rev. B* **1999**, *60*, 13339−13342.

(9) Takenobu, T.; Takano, T.; Shiraishi, M.; Murakami, Y.; Ata, M.; Kataura, H.; Ashiba, Y.; Iwasa, Y. *Nat. Mater.* **2003**, *2*, 683−688.

(10) Lee, R. S.; Kim, H. J.; Fisher, J. E.; Thess, A.; Smalley, R. E. *Nature (London)* **1997**, *388*, 255−257.
(11) Rao, A. M.; Richter, E.; Bandow, S.; Chase, B.; Eklund, P. C.; Williams, K. A.; Fang, S.; Subbaswamy, K. R.; Menon, M.; Thess, A.; Smalley, R. E.; Dresselhaus, G.; Dresselhaus, M. S. *Science* **1997**, *275*, 187−190.
(12) Liu, X.; Pichler, T.; Knupfer, M.; Fink, J. *Phys. Rev. B* **2003**, *67*, 125403.
(13) Strano, M. S.; Huffman, C. B.; Moore, V. C.; O'Connell, M. J.; Haroz, E. H.; Hubbard, J.; Miller, M.; Rialon, K.; Kittrell, C.; Ramesh, S.; Hauge, R. H.; Smalley, R. E. *J. Phys. Chem. B* **2003**, *107*, 6979−6985.
(14) Itkis, M. E.; Niyogi, S.; Meng, M. E.; Hamon, M. A.; Hu, H.; Haddon, R. C. *Nano Lett.* **2002**, *2*, 155−159.
(15) Grigorian, L.; Williams, K. A.; Fang, S.; Sumanasekera, G. U.; Loper, A. L.; Dickey, E. C.; Pennycook, S. J.; Eklund, P. C. *Phys. Rev. Lett.* **1998**, *80*, 5560−5563.
(16) Skákalová, V.; Dettlaff-Weglikowska, U.; Roth, S. *Diamond Relat. Mater.* **2004**, *13*, 296−298.
(17) Hennrich, F.; Wellmann, R.; Malik, S.; Lebedkin, S.; Kappes, M. *Phys. Chem. Chem. Phys.* **2003**, *5*, 178−183.
(18) Terrones, M.; Jorio, A.; Endo, M.; Rao, A. M.; Kim, Y. A.; Hayashi, T.; Terrones, H.; Charlier, J. C.; Dresselhaus, G.; Dresselhaus, M. S. *Materials Today*, October 2004, pp 30−45.
(19) Chiu, P. W.; Duesberg, G. S.; Dettlaff-Weglikowska, U.; Roth, S. *Appl. Phys. Lett.* **2002**, *80*, 3811.
(20) Dettlaff-Weglikowska, U.; Skakalova, V.; Graupner, R.; Ley, L.; Roth, S. *AIP Conf. Proc.* **2003**, *685*, 277.
(21) Holzinger, M.; Vostrowsky, O.; Hirsch, A.; Hennrich, F.; Kappes, M.; Weiss, R.; Jellen, F. *Angew. Chem., Int. Ed.* **2001**, *40*, 4002.
(22) Bachilo, S. M.; Strano, M. S.; Kittrell, C.; Hauge, R. H.; Smalley, R. E.; Weisman, R. B. S*cience* **2002**, *298*, 2361.
(23) Strano, M. S.; Doorn, S. K.; Haros, E. H.; Kittrell, C.; Hauge, R. H.; Smalley, R. E. *Nano Lett.* **2003**, *3*, 1091.
(24) Zheng, M.; Jagota, A.; Semke, E. D.; Diner, B. A.; McLean, R. S.; Lustig, S. R.; Richardson, R. E.; Tassi, N. G. *Nat. Mater.* **2003**, *2*, 338.
(25) Chattopadhyay, D.; Galeska, I.; Papadimitrakopoulos, F. *J. Am. Chem. Soc.* **2003**, *125*, 3370.
(26) Strano, M. S.; Dyke, C. A.; Usrey, M. L.; Barone, P. W.; Allen, M. J.; Shan, H.; Kittrell, C.; Hauge, R. H.; Tour, J. M.; Smalley, R. E. *Science* **2003**, *301*, 1519−1522.
(27) Hu, H.; Zhao, B.; Hamon, M. A.; Kamaras, K.; Itkis, M. E.; Haddon, R. C. *J. Am. Chem. Soc.* **2003**, *125*, 14893−14899.
(28) Kavan, L.; Rapta, P.; Dunsch, L.; Bronikowski, M. J.; Willis, P.; Smalley, R. E. *J. Phys. Chem. B* **2001**, *105*, 10764−10771.
(29) Wu, Z.; Chen, Z.; Du, X.; Logan, J. M.; Sippel, J.; Nikolou, M.; Kamaras, K.; Reynolds, J. R.; Tanner, D. B.; Hebard, A. F.; Rinzler, A. *Science* **2004**, *305*, 1273.
(30) Heller, D. A.; Barone, P. W.; Swanson, J. P.; Mayrhofer, R. M.; Strano, M. S. *J. Phys. Chem. B* **2004**, *108*, 6905−6909.
(31) Rao, A. M.; Eklund, P. C.; Bandow, S.; Thess, A.; Smalley, R. E. *Nature (London)* **1997**, *388*, 257−259.
(32) Brown, S. D. M.; Jorio, A.; Corio, P.; Dresselhaus, M. S.; Dresselhaus, G.; Saito, R.; Kneipp, K. *Phys. Rev. B* **2001**, *63*, 155414−1−155414−8.
(33) Kaiser, A. B.; Düsberg, G.; Roth, S. *Phys. Rev. B* **1998**, *57*, 1418−1421.
(34) Kaiser, A. B. *Rep. Prog. Phys.* **2001**, *64*, 1−49.
(35) Rogers, S. A.; Kaiser, A. B. *Curr. Appl. Phys.* **2004**, *4*, 407−410.
(36) Shiraishi, M.; Ata, M. *Synth. Met.* **2002**, *128*, 235−239.
(37) Pietronero, L. *Synth. Met.* **1983**, *8*, 225−231.
(38) Sheng, P. *Phys. Rev. B* **1980**, *21*, 2180−2195.